Available online at www.sciencedirect.com
ScienceDirect
C. R. Geoscience 340 (2008) 883–892
COMPTES RENDUS GEOSCIENCE
http://france.elsevier.com/direct/CRAS2A/

Surface geosciences (palaeoenvironment)

Late Glacial-Holocene sequence of Lake Saint-Point (Jura Mountains, France): Detrital inputs as records of climate change and anthropic impact

Aurélie Leroux [a,*], Vincent Bichet [a], Anne-Véronique Walter-Simonnet [a], Michel Magny [a], Thierry Adatte [b], Émilie Gauthier [a], Hervé Richard [a], Agnès Baltzer [c]

[a] *Laboratoire chrono-environnement, UMR CNRS 6249, université de Franche-Comté, 16, route de Gray, 25030 Besançon cedex, France*
[b] *Institut de géologie, université de Neuchâtel, 11, rue Émile-Argand, 2007 Neuchâtel, Suisse*
[c] *Laboratoire de morphologie continentale et côtière, UMR 6143 M2C, université de Caen, 24, rue des Tilleuls, 14032 Caen cedex, France*

Received 23 May 2008; accepted after revision 12 August 2008
Available online 11 October 2008

Presented by Georges Pédro

Abstract

A sediment sequence (SP05, 12.5 m long) was taken from the deep zone of Lake Saint-Point (850 m a.s.l.). Sedimentological analyses highlight two main contrasted periods of sedimentation: the Last Glacial Maximum (LGM)/Late Glacial characterized by high silicates and quartz contents the Holocene dominated by the carbonated fraction. At the beginning of the Holocene (11 400 years cal. BP), silicates fraction flux abruptly decreased. The shift between the Late Glacial and the Holocene periods may be explained by forest development in the catchment. From 10 200 to 6800 years cal. BP, silicates and detrital carbonate fractions remained stable before they progressively increased steady till 5000 years cal. BP. Both increases cannot be totally attributed to an anthropic impact since pollen data indicate continuous anthropic activities only dated back from 3000 years cal. BP. They thus resulted from a dominant climatic control. From 5000 years cal. BP, silicates content still increased while detrital carbonates input became steady due to a change in pedogenetic processes affecting the catchment. During the last millennium, silicates and detrital carbonate decreased, probably due to pastureland development. ***To cite this article: A. Leroux et al., C. R. Geoscience 340 (2008).***

Résumé

La séquence Tardiglaciaire-Holocène du Lac Saint-Point (Jura, France) : le détristisme, indicateur des changements climatiques et de l'impact anthropique. Une séquence sédimentaire (SP05, 12,5 m de long) a été forée dans la partie profonde du Lac Saint-Point (850 m a.s.l.). Les analyses sédimentologiques mettent en évidence deux périodes de sedimentation : le Pléniglaciaire/Tardiglaciaire, caractérisé par d'importantes teneurs en silicates et quartz et l'Holocène dominé par la sédimentation carbonatée. Au début de l'Holocène, les flux de silicates et de carbonates détritiques décroissent brutalement à la suite du développement de la forêt dans le bassin versant. De 10 200 à 6800 ans cal. BP, les apports silicatés et le détritisme carbonaté sont stables, puis augmentent régulièrement jusqu'à 5000 ans cal. BP. Ces augmentations ne peuvent être entièrement assimilées à

* Corresponding author.
E-mail address: aurelie.leroux@univ-fcomte.fr (A. Leroux).

1631-0713/$ – see front matter
doi:10.1016/j.crte.2008.08.005

un impact anthropique, puisque les données polliniques indiquent une activité anthropique continue, seulement à partir de 3000 ans cal. BP. Le contrôle climatique apparaît dominant. À partir de 5000 ans cal. BP, les apports silicatés augmentent, alors que le détritisme carbonaté se stabilise. Ce phénomène est la conséquence d'un changement de pédogenèse au sein du bassin versant. Vers 1000 ans cal. BP, silicates et carbonates détritiques décroissent probablement en raison du développement de pâturages. ***Pour citer cet article : A. Leroux et al., C. R. Geoscience 340 (2008).***

Keywords: Lake; Detristism; Holocene; Carbonates; Anthropic; Climate

Mots clés : Lac ; Détritisme ; Holocène ; Carbonates ; Anthropique ; Climat

1. Introduction

Lake archives currently provide us with amongst the most continuous record of climate changes affecting continental areas since the Last Glacial Maximum (LGM). These geosystems are both directly influenced by human impact and global climate change. Lacustrine sediments, therefore, enable us to distinguish between global and local climate change effects. Besides, even if Jurassian lakes have been largely investigated for climate record, these investigations were conducted most of the time on records taken from the littoral areas [13,14] often affected by sediment hiatuses. Few studies were carried out on sedimentological features of sequences taken from deep part of lakes [2,20,25], although they provide continuous records without hiatus and, through high-resolution sedimentological studies, document both environmental and climatic changes. Due to its morphological features, potential infill and sensitive location close to the summit area of Jura Mountains, Lake Saint-Point appears to be an appropriate site for this kind of investigation, and notably for high resolution detrital inputs (silicates and carbonates) studies.

2. Geographical and geological settings

Lake Saint-Point (46°48.7 N, 6°12.2 E; 850 m a.s.l.) is located in the high chain of Jura Mountains. This lake (7 km^2) is divided into two basins separated by a sill located at a depth of 21.5 m (Fig. 1). Depths in the upstream and downstream basins respectively reach 41 m and 35.5 m. The lake's shape is forced by the synclinal structure of the Doubs Valley and the retreat of the LGM ice cap [5]. Lake Saint-Point is fed by the Doubs River, which supplies the main part of the suspended matter. Altitudes of its catchment (247 km^2) range from 850 to 1463 m a.s.l (Mont D'Or) (Fig. 1). In this area, detritism-supplying geological layers correspond to Late Jurassic and Upper Cretaceous carbonates formations. In this context, lacustrine sedimentation is clearly dominated by both detrital and authigenic carbonates [2].

3. Material and methods

Prior to the coring, a seismic survey (seistec IKB high resolution) was carried out in order to highlight disturbance zones (slumps). Then, using seismic profiles, a continuous sequence (SP05; 12.5 m long) was cored in the central and deepest part of the downstream basin, at a depth of 35.5 m (Fig. 1). A coring platform (UWITEC system) was used to acquire the sequence SP05, which enabled us to extract 3-m long sections. Twin cores were taken in order to avoid problems linked to the transition between sections. Using these twin sections as well as correlations of obvious markers (lithofacies, laminae, tephra layers), a master core was reconstructed.

Chronology of the sequence is based on 24 AMS radiocarbon dates (Table 1) spread over the upper 7 m of the core. Under 7 m depth, no matter was available for radiocarbon datation. All the dates were determined thanks to leaves and wood fragment analyses, and calibrated using the program CALIB 5.1 [19]. The chronology was completed by pollen analysis made on punctual samples (regional pollen stratigraphy), particularly for the oldest part of the sequence (Oldest Dryas limits), and by the geochemical and mineralogical identification of the Laacher See Tephra (LST) [4,9,23,24]. Another tephra was observed during the Early Holocene but remains non-identified because of the size of the volcanic shards, which hampers any chemical analysis with electron microprobe techniques. Nevertheless, its chronological position could be compatible with the Early Holocene Vasset-Killian eruption, from the Massif Central, which has been recently described in Switzerland [3].

Concerning the recent period, ^{137}Cs measurements [16,21] were processed on the 20 upper centimetres of the sequence. Pollen analysis is currently still in

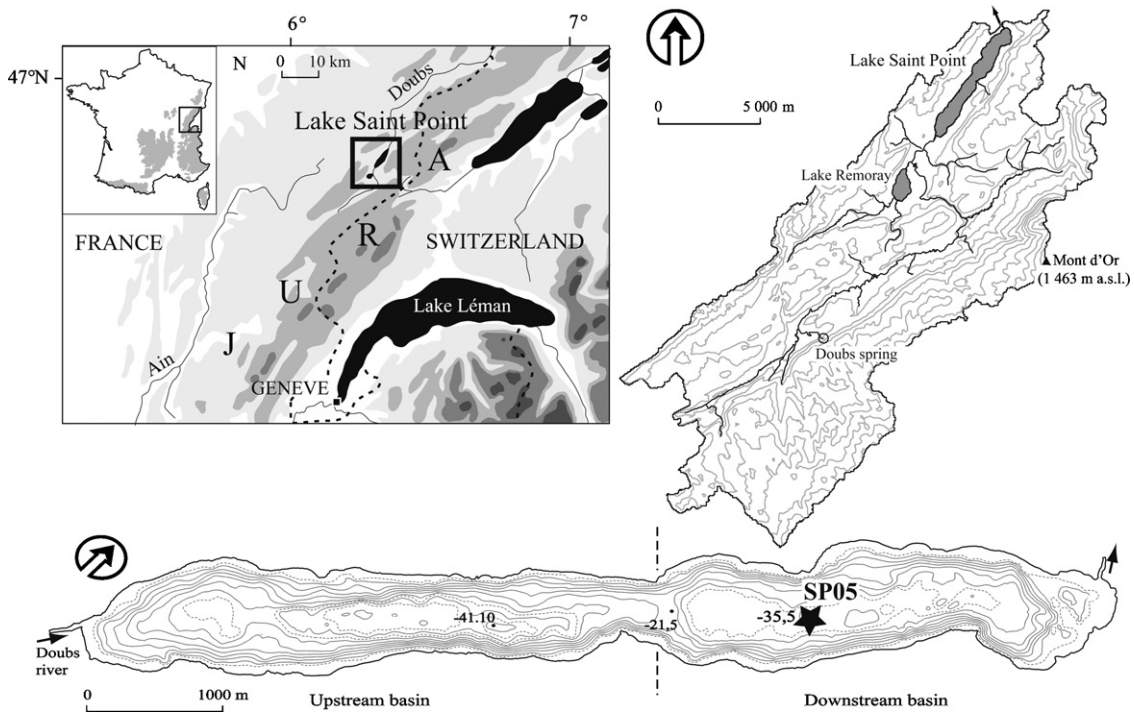

Fig. 1. Location of Lake Saint-Point; topographic map of its catchment; bathymetric map and location of the core.
Localisation du Lac Saint-Point ; carte topographique du bassin versant ; carte bathymétrique et localisation du forage.

progress; therefore, only mid- and late Holocene data is presented in this paper.

Physical parameters (gamma density and magnetic susceptibility [MS]) were measured using a Geotek Multi Sensor Core Logger System with a step of 5 mm.

The bulk sediment was analysed for grain size analysis (laser granulometer, LS230 Beckman-Coulter), major elements contents (XRF) and mineralogy (DRX). The sampling step was adjusted to the depth-age model but due to the condensation of some periods, its temporal resolution ranges from 60 to 200 years/sample (Fig. 2) with a resolution lower than 100 years for the Holocene.

4. Results

4.1. Depth-age model

The sequence documents the sedimentation from LGM (sensu lato) to current period (Fig. 2). Sedimentation rates greatly vary but stay between 0.07 mm years^{-1} (11 400–10 200 years cal. BP) and 3.1 mm years^{-1} (Modern period). The depth-age curve (Fig. 2) indicates quite similar sedimentation rates during the Late Holocene (from 6000 years cal. BP) as well as from 18 300–15 000 years cal. BP (Oldest Dryas). Very low sedimentation rates are observed from 15 000 to 10 200 years cal. BP (from the Bølling to the end of the Preboreal) prior to an increase beginning in 500 years cal. BP (the end of Late Atlantic pollen zone). The lowest sedimentation rates occur during the time interval 11 400–10 200 years cal. BP. Except for this particular period, sedimentation rates appear to be quite steady during the Holocene. Nevertheless, two increases are observed at 10 200 years cal. BP and 5400 years cal. BP. As for the highest sedimentation rates, they are recorded during the last century.

4.2. Sedimentological features

Based on sedimentological features, the sequence can be divided in six units showing very different colours (Fig. 2). Units 1 and 2 (U1 and U2) cover the end of LGM and the beginning of Late Glacial (till 15 000 years cal. BP-Oldest Dryas pollen zone). These well-laminated units are characterized by the presence of sandy levels which are not observed in other units. Unit 3 (U3) represents a very condensed sequence, spanning from 15 000 to 10 200 years cal. BP (from Bølling to the Boreal pollen zones). In this unit, the LST corresponds to a thin greyish level well known in other regional lacustrine records [4,11,24]. Unit 4 (U4) is a

Table 1
AMS radiocarbon dates ^{137}Cs results obtained from core SP05
Datations AMS radiocarbon et résultats du ^{137}Cs obtenus à partir de la carotte SP05

Daiations methods	Depth (cn)	Radiocarbon date (BP)	Ages 2σ range (y cal. BP)	Laboratory reference	Material
^{137}Cs	6.5	–	−36(1986)	–	Bulk sediment
^{137}Cs	10.5	–	−13(1963)	–	Bulk sediment
^{14}C	125	1120 ± 30	956–1088	Poz-17040	Leaves
^{14}C	126.5	1100 ± 30	952–1062	Poz-17041	Leaves
^{14}C	127.5	1155 ± 30	979–1150	Poz-17041	Leaves
^{14}C	157.4	1775 ± 35	1604–1817	Poz-17043	Leaves
^{14}C	157.6	1785 ± 35	1613–1818	Poz-17051	Leaves
^{14}C	185	2145 ± 35	2033–2305	Poz-17055	Leaves
^{14}C	190.5	2230 ± 35	2152–2336	Poz-17057	Leaves
^{14}C	192.5	2255 ± 35	2155–2344	Poz-17068	Leaves
^{14}C	193.5	2195 ± 35	2124–2324	Poz-17053	Leaves
^{14}C	198.5	2490 ± 30	2457–2725	Poz-17054	Twigs
^{14}C	219.5	2800 ± 35	2839–2993	Poz-17067	Leaves
^{14}C	220	2975 ± 35	3059–3319	Poz-17065	Leaves
^{14}C	246.5	3360 ± 35	3483–3689	Poz-17064	Leaves
^{14}C	250.5	3500 ± 35	3688–3871	Poz-17062	Leaves
^{14}C	271.5	3740 ± 35	3982–4160	Poz-17063	Needle
^{14}C	278.5	3935 ± 35	4281–4513	Poz-17061	Leaves
^{14}C	290.5	4130 ± 35	4566–4821	Poz-17060	Leaves
^{14}C	306.5	4460 ± 40	4960–5294	Poz-17059	Leaves
^{14}C	337.5	4850 ± 40	5476–5657	Poz-18354	Leaves
^{14}C	352.5	5150 ± 50	5748–5995	Poz-18356	Leaves
^{14}C	483	6500 ± 50	7308–7507	Poz-18353	Leaves
^{14}C	484	6470 ± 50	7276–7461	Poz-18357	Leaves
^{14}C	501	6980 ± 50	7695–7932	Poz-18315	Leaves
^{14}C(LST)[9]	671	11 230 ± 40	13 125 ± 560	–	Terrestrial macrofossils
^{14}C	683	11 730 ± 60	13 426–13733	60	Leaves

very particular facies made of unlaminated lacustrine chalk corresponding to the first half of the Holocene (8900–5400 years cal. BP). Units 5 and 6 (U5 and U6) can be eventually distinguished due to their organic matter content, which is higher than in the preceding units (C_{org}, Fig. 3).

The gamma density shows a progressive decrease with time, with two discreet shifts at the LGM-Late Glacial and Late Glacial-Holocene transitions (Fig. 3). The MS signal is characterized by two increasing trends separated by a strong decrease occurring during the interval 11 400–10 200 years cal. BP (Preboreal pollen zone) (Fig. 3). The two peaks observed correspond to tephra layers. Grain size analyses show that the thin (< 50 μm) fraction is dominant (Fig. 3). The coarser fraction (> 50 μm) sometimes appears during the Late Glacial but is observed all along from 6800 years cal. BP to the current period, with a progressive increase in U5 unit followed by a slight decrease at the top of U6 unit corresponding to the present time.

The mineralogy (Fig. 3) is clearly dominated by calcite (50 to 99%) associated to quartz and clay minerals, dolomite, plagioclase and feldspars only featuring as accessory minerals (less than 3%). From the LGM to 11 400 years cal. BP, calcite evolution (Fig. 3) appears to remain quite steady and increases from 11 400 years cal. BP on (Preboreal). The first half of the Holocene (11 400–5400 years cal. BP) is characterized by the highest calcite content. As for its second half, it shows a decreasing trend followed by another calcite content rise during the last millennium. These main periods are also emphasized by quartz content evolution (Fig. 3). From the LGM to 11 400 years cal. BP, quartz content shows pulses of high quartz inputs reaching about 20%. Quartz content is higher during Late Glacial than during the LGM. By contrast, no quartz input occurs during the first half of the Holocene (apart from two peaks at around 9000 years cal. BP). From 6500 years cal. BP on, quartz content increases but its proportion (∼3%) remains lower than those observed during the previous periods, except for the most recent period.

4.3. Geochemical features

The relations between Ca and Sr concentrations were used to characterize carbonates assemblages (Fig. 4).

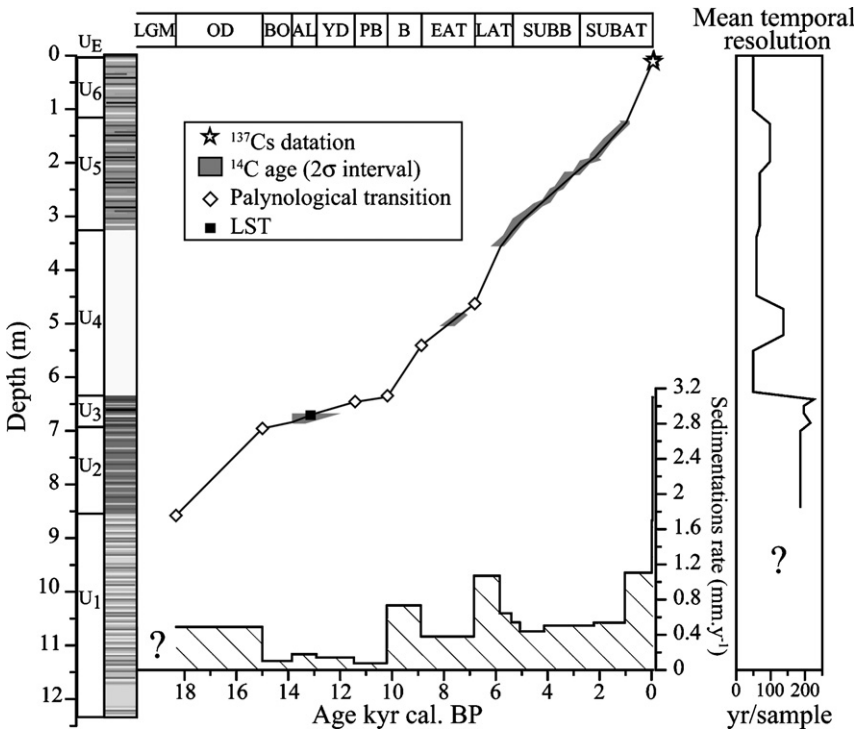

Fig. 2. Age-depth model and sedimentation rates obtained from the different datation methods; sedimentological units; evolution of sample temporal resolution (LGM: Last Glacial Maximum [sensu lato]; OD: Oldest Dryas; BO: Bølling; AL: Allerød; YD: Younger Dryas; PB: Preboreal; B: Boreal; EAT: Early Atlantic; LAT: Late Atlantic; SUBB: Subboreal; SUBAT: Subatlantic).

Modèle âge-profondeur et taux de sédimentation obtenus à partir des différentes méthodes de datation ; unités sédimentologiques ; variation de la résolution temporelle des échantillons (LGM : dernier maximum glaciaire ; BO : Bølling ; AL : Allerød ; YD : Dryas récent ; PB : Préboréal ; B : Boréal ; EAT : Atlantique ancien ; LAT : Atlantique récent ; SUBB : Subboréal ; SUBBAT : Subatlantique).

Their relations point out two different carbonated populations associated respectively to LGM/Late Glacial period and to the Holocene. The LGM/Late Glacial carbonates are characterized by high Sr values, whereas Holocene carbonates present lower Sr content. The correlations observed between Al_2O_3 and SiO_2 also shows the occurrence of two silicated populations, associated to the same periods as observed in the carbonate fractions (Fig. 5). From the LGM to the Preboreal (11 400 years cal. BP), samples are richer in silica and poorer in alumina than Holocene ones.

The proportions of the different fractions (carbonates, silicates, organic carbon) were reconstructed from major elements analyses and LOI. Assuming that the Ca is mainly associated to the carbonate fraction, it is possible to work out the total carbonates content. The LOI. corresponds both to $CaCO_3$ and organic matter, thus organic carbon can be worked out from LOI. measurement after correction of $CaCO_3$ content. Silicate fraction was eventually calculated as the remaining fraction. The worked-out carbonate evolution is consistent with the calcite variations (Fig. 3) and shows a major transition at around 11 000 years cal. BP. The organic fraction rises up at 6000 years cal. BP but still remains lower than 5%. The silicate fraction is comprised between 4 and 45% (Fig. 3) and characterized by the same main variations as that of quartz content.

Major elements analyses were also used to calculate the CIA (chemical index of alteration, CIA = Al/(Al + K + Na + Ca*) in which Ca* corresponds to the plagioclase, negligible in this context) [15]. This indicator of pedogenetic alteration underlines three main periods (Fig. 3). From the LGM to the Preboreal (11 400 years cal. BP), the CIA slightly decreases and shows high variations from 10 200 years cal. BP to 6800 years cal. BP. A continuous increase occurs from 6800 years cal. BP prior to a slow decrease until the Modern period. From the last millennium on, its variation appears quicker and more important.

4.4. Detrital carbonate input calculation

Mg is associated to the detrital carbonates coming from catchment (Doubs water composition only enables

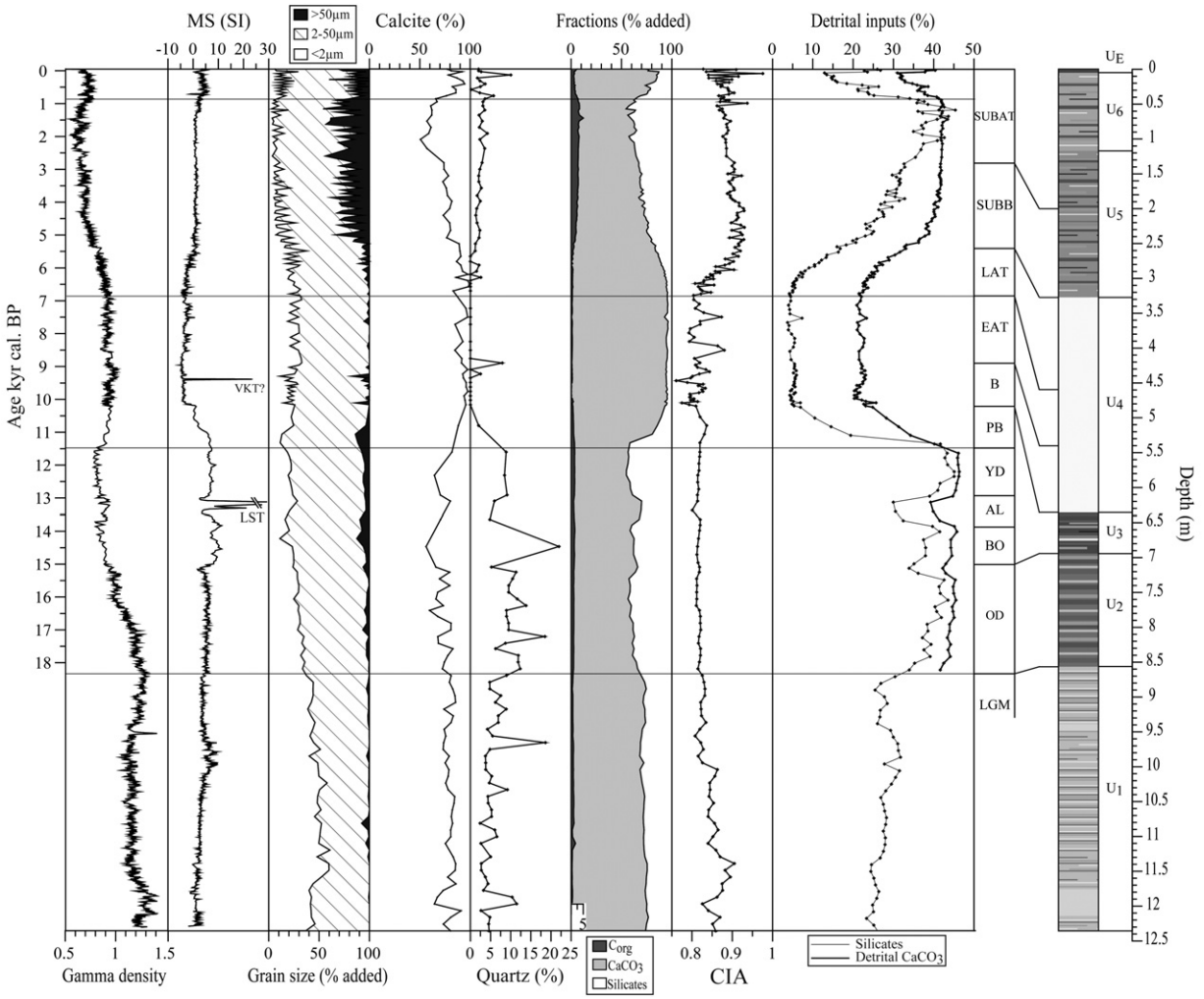

Fig. 3. Sedimentological features: MS (for magnetic susceptiblility) and gamma density were measured using a Geotek Multi Sensor Core Logger System; calcite and quartz % resulted from DRX analysis; The carbonates, C_{org} and silicate contents were calculated thanks to major elements analyses results; CIA: Chemical Index of alteration; the detrital carbonates flux were worked out using Mg–Ca content. The horizontal lines indicate main sedimentological transitions.

Caractéristiques sédimentologiques ; MS et gamma densité ont été mesurés à l'aide d'un Geotek Multi Sensor Core Logger System ; les pourcentages en calcite et quartz résultent de l'analyse DRX sur roche totale ; les pourcentages en carbonates, C_{org} et silicates ont été calculés à partir des résultats de l'analyse des éléments majeurs ; CIA : indice d'altération chimique ; le flux de carbonates détritiques a été calculé à partir des teneurs en Ca–Mg. Les repères horizontaux indiquent les transitions sédimentologiques majeures.

the precipitation of pure calcite or very low-Mg calcite [6]) and, as a consequence, it is used as an indicator of detrital carbonates input.

Since the plagioclase and dolomite inputs are negligible from the Late Glacial onwards, the detrital carbonate input was worked out using the linear regressions observed between Ca and Mg (Fig. 6). The Ca content of theoretical authigenic carbonates was calculated for the different periods. Assuming that the detrital carbonate pool corresponds to the highest Mg contents, the composition of the detrital carbonate pool was calculated using chemical data together with chemical analyses of the catchment rocks [1] (Fig. 6). Then, compositions of theoretical authigenic (Ca_a) and detrital carbonates (Ca_d) pools, and Ca content in samples (Ca_s), were used to determine proportions of each fraction through a two components mixture calculation: $Ca_s = f \times Ca_a + (1- f) \times Ca_d$ where f is the proportion of Ca_a in the mixture [12].

The inputs of silicates and detrital carbonates (Fig. 3) underline the major transition previously observed. During the LGM and the Late Glacial, detrital inputs are high and represent around 80% of the sedimentation. These fluxes increase at the beginning

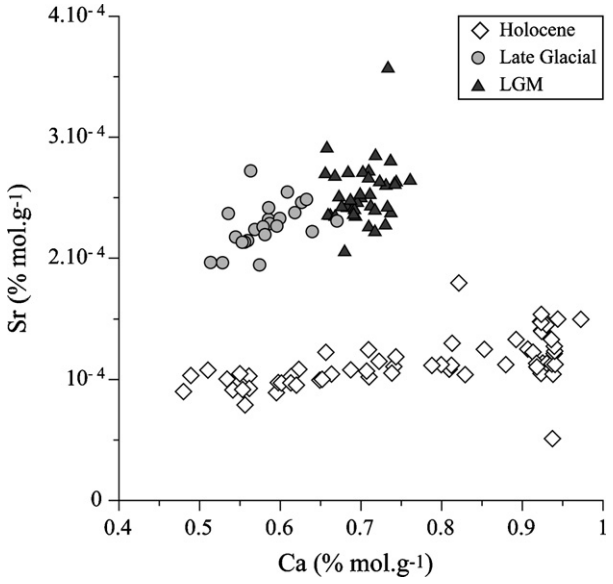

Fig. 4. Relation between Ca and Sr concentrations (bulk sediment) expressed by periods (Sr-values were acquired by ICPMS analysis on bulk sediment).
Relation entre les concentrations en Ca et Sr (roche totale) selon les périodes (les valeurs Sr ont été obtenues par analyse ICPMS sur roche totale).

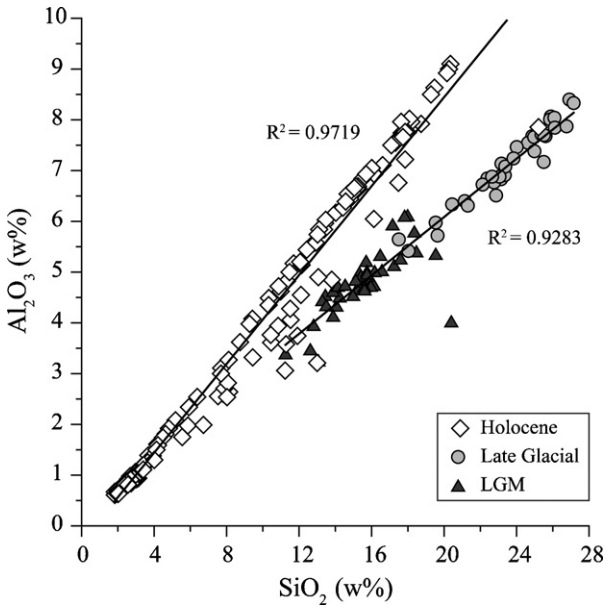

Fig. 5. Linear relations between Al_2O_3 and SiO_2 (bulk sediment) expressed by periods.
Corrélations linéaires entre les teneurs en Al_2O_3 et SiO_2 (roche totale) selon les périodes.

of Late Glacial (18 300 years cal. BP). At 11 400, detrital inputs steeply drop, but the silicate input remains lower than the detrital carbonate one. At least, detritism rises up from 6800 years cal. BP reaching

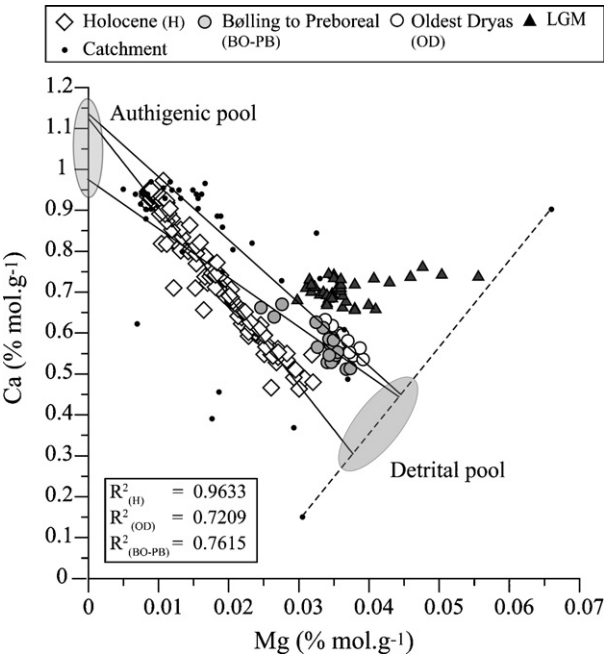

Fig. 6. Linear correlations between Ca and Mg expressed by periods. The equations of linear regression supply the Ca-values of theoretical authigenic pools. The detrital pools were determined as the cross section between the linear regressions and the Ca–Mg limit composition from catchment samples.
Corrélations linéaires entre Ca et Mg suivant les périodes. Les équations des régressions linéaires fournissent les valeurs Ca des pôles de carbonates théoriques. Les pôles détritiques ont été déterminés comme étant les points d'intersection entre les régressions linéaires et la composition limite en Ca–Mg des échantillons du bassin versant.

ca 70% before decreasing again during the last millennium.

4.5. Pollen data (from 7500 years cal. BP to recent period)

Presently, the first results in pollen analysis (Fig. 7) document the last 7500 years. Arborean pollen (AP) appears to be dominant (around 90%) throughout the whole sequence. Nevertheless, the proportion of AP pollen decreases from 3000 years cal. BP with a main drop from 1400 years cal. BP on. At 6800 years cal. BP, a change in vegetation assemblage is underlined through a change in the dominant species corresponding to the transition between early Atlantic and late Atlantic. Indeed, *Quercus mixed* decreases in favour of *Abies* and *Picea*. The drop of AP is synchronous with the main increasing phases underlined by anthropic indicators (AI, defined as the sum of *Cerealia, Apophytes, Juniperus* and *Cannabis*) (Fig. 7).

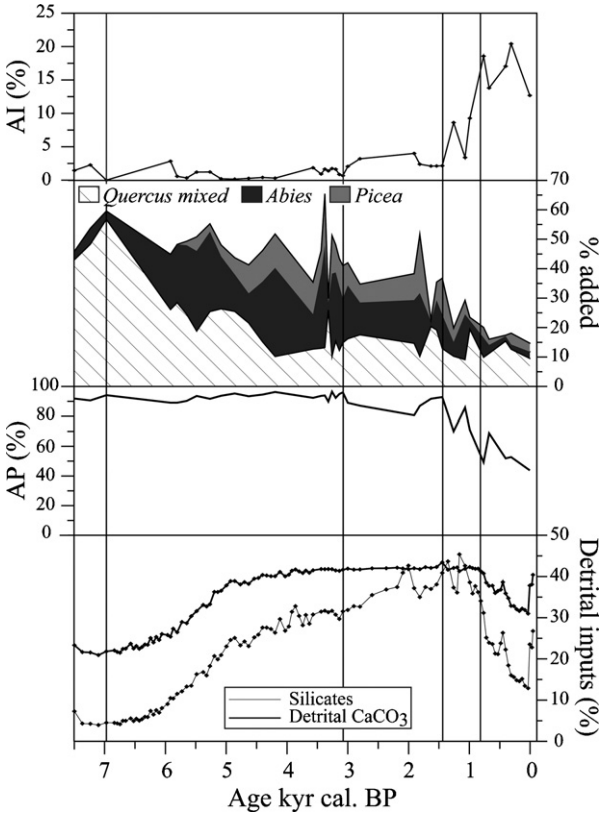

Fig. 7. Detrital inputs compared to pollen data spanning from 7500 years cal. BP to Modern period; AP: arborean pollen; AI: anthropic pollen indicators (*Cerealia, Apophytes, Juniperus* and *Cannabis*).
Apports détritiques comparés aux données palynologiques couvrant les derniers 7500 ans cal. BP ; AP : pollen d'arbres ; AI : indice pollinique d'anthropisation (Cerealia, Apophytes, Juniperus and Cannabis).

5. Discussion

5.1. The LGM-Late Glacial transition (18 200 years cal. BP)

Prior to the Holocene, the carbonate signature is dominated by the catchment bedrock (Fig. 4). High quartz input may be partly inferred to bedrock insoluble residue and allochtonous inputs (Fig. 3). Indeed, previous studies [18,25] highlighted aeolians inputs in the Jura and in central Europe until the end of the Oldest Dryas. Considering no soil development affected the catchment during LGM due to the presence of the ice cap, the high CIA values indicate Lake Saint-Point was fed by aeolian soil particles reworked and mixed to the products of bedrock erosion. The slight decrease in CIA values from the LGM to the Late Glacial, may be explained as the erosion of older soils formed during the previous interstadial. From 18 300 years cal. BP, the increases in quartz content and silicate inputs are the consequences of the deglaciation through a change in water input and the outcropping of new areas where aeolian particles deposited. According to Buoncristiani and Campy [5], we infer that a transition from a subglacial position to a free of ice position of Lake Saint-Point took place at ca 18 300 years cal. BP.

5.2. The Late Glacial-Holocene transition (11 400 years cal. BP)

The second part of the Late Glacial (from 15 000 to 11 400 years cal. BP) is characterized by the lowest sedimentation rates (Fig. 2) probably due to a very low authigenic production and the depletion of the deglaciation products, although detrital contributions remain high (80%, Fig. 3). In contrast with this preceding period, the beginning of the Holocene corresponds to a steep drop in detritism fluxes and an increase in sedimentation rates (Figs. 2 and 3). These evolutions involve a huge increase in authigenic carbonate production at ca 10 200 years cal. BP. The low-Sr values in carbonates (Fig. 4) observed during the Holocene confirm this assumption. The high frequency CIA variation (Fig. 3) and the enrichment in Al_2O_3 (Fig. 5) indicate more efficient and active pedogenetic processes in the catchment. This evolution is the consequence of the forest development directly subsequent to the beginning of the Holocene warming. Indeed, previous palynological studies [7,17], mentioned a rapid transition from a steppe (Younger Dryas) to a forest composed by mesothermophile species (e.g. *Pinus* and *Betula*) at the Preboreal (11 400–10 200 years cal. BP). As a consequence, the erosion became less efficient [22]. Moreover, this period corresponds to an important hydrologic crisis in different Jurassian lakes with low lake-levels [13] and reduction of detritism [2]. The huge decrease in quartz flux (Fig. 3) is probably the consequence of the aeolioan depletion. This transition appears as a main change in environmental and climatic conditions.

5.3. The Late Holocene variations (6800 years cal. BP to the actual period)

The environmental change occurring at 6800 years cal. BP appears more continuous than those observed at the beginning of Late Glacial and Holocene periods (Fig. 3). Both detrital inputs rise up from 6800 years cal. BP on. However, silicate input evolves faster than detrital carbonate input (Fig. 3). This evolution is obviously present in the CIA variation, which indicates

a more efficient chemical alteration in the catchment through an increase in the index. A change in pollen assemblage occurred whereas pollen data do not indicate any change in forest importance (AP > 80%, Fig. 7). *Abies* and *Picea* develop at the expense of mixed oak forest (*Quercus* mixed, Fig. 7); this modification cannot be solely attributed to human activities as demonstrated by the low and punctual AI values (< 2.5%) (Fig. 7), but is probably the consequence of cooler climatic conditions [8]. Some previous palynological study in the area [7] at the same altitude, notably at Lake Remoray (Fig. 1), actually pointed out no large-scale human impact on the environment at the same period. This detritism evolution is the consequence of the change from a deciduous to a resinous forest through a change in soil production. *Abies* and *Picea* generate larger and more acidic soils enhancing carbonates dissolution, which enables the residual quartz concentration in soil and, thus, explains the increase in quartz content (Fig. 3). As a consequence, the carbonate dissolution efficiency and therefore detrital carbonates flux depend on the erosion rate. This explains the contrast observed between variations in detrital carbonate and silicate inputs which follows the *Abies* development. Besides, an increase in silicate input occurs and goes on after 3100 years cal. BP. According to a lake level and glacier fluctuation study [10], this period is characterised by an advance of alpine glaciers at ca 3000 years cal. BP consistent with high lake level in Jura Mountains, indicating an increase in hydrologic flux. This climatic reversal enhances detritism flux. Nevertheless, AI and AP (Fig. 7) start to rise up and to drop respectively at the same period. Deforestation and agricultural exploitation are also factors enhancing detritism. In this context, the increase in silicate input is the consequence of both anthropic and climatic effects.

Although the first continuous indicators for human activities pointed out by AP and AI appear at 3000 years cal. BP, they indicate a huge human development only from 1400 years cal. BP (Fig. 7). This anthropic impact progressively induces the covariation of both detrital fluxes and their decrease. This particular evolution of detrital input corresponds to a land use change through the development of pasturelands at the expense of cultivated areas (increase in *Apophytes*). Hence, we may consider human activities as the main factor for environmental change during the last millennium.

6. Conclusion and perspectives

The Lake Saint-Point provides a continuous sequence enabling the characterisation of the main climatic and environmental changes from the LGM to the actual period. This sequence underlines three different evolutions of detrital inputs directly/indirectly triggered by climate change and/or anthropic effect.

The Late Glacial transition corresponds to an increase in hydrologic fluxes due to the deglaciation. As a consequence, sedimentation is characterized by high detritism and an important contribution of eaolian particles (huge quartz content). The beginning of the Holocene indicates a drop of detrital carbonates and silicate inputs. This period corresponds to the huge forest cover development observed in different Jurassian areas directly subsequent to the Holocene warming. The 6800 years cal. BP transition highlights the rise up of detrital inputs associated to a change in pollen assemblage. This period corresponds to the development of *Abies* at the expense of *Quercus*, thereby inducing a change in pedogenetic processes and thus a change in silicate production. Considering the low value of AI, the *Abies* development is probably the consequence of cooler climatic conditions. The last millennium is the most affected by human activities (as demonstrate by AI increase) despite the overall decrease in detrital inputs. This particular evolution is the consequence of a land use change through the development of pasturelands over previously cultivated areas.

Considering the different results, vegetation changes appear as the main factors of change in sedimentation feature through their natural or anthropic modification. The reconstruction of detrital carbonates requires taking into account pedogenetic processes. Silicates detritism flux eventually must be carefully interpreted in carbonates system.

Acknowledgments

This work was supported by the City of Besançon and the CNRS JurAlp project. We thank M. Desmet and the Edytem Laboratory (Chambéry) for supplying the coring platform. We also thank P. Capiez for XRF analyses and J.-P. Simonnet for his precious help in granulometry analysis.

References

[1] V. Bichet, Impact des contraintes environnementales sur la production sédimentaire d'un bassin versant jurassien au cours du Post-Glaciaire : le système limnologique de Chaillexon (Doubs, France), Ph.D. thesis, Université de Bourgogne, 1997, 206 p.

[2] V. Bichet, M. Campy, J.-F. Buoncristiani, C. Digiovanni, M. Meybeck, H. Richard, Variations in Sediment Yield from the

upper Doubs River Carbonate Watershed (Jura, France) since the Late-Glacial Period, Quat. Res. 51 (1999) 267–279.

[3] S.P.E. Blockley, C.S. Lane, A.F. Lotter, A.M. Pollard, Evidence for the presence of the Vedde Ash in Central Europe, Quat. Sci. Rev. 26 (2007) 3030–3036.

[4] G. Bossuet, H. Richard, M. Magny, M. Rossy, Nouvelle occurrence du Laacher See Tephra dans le Jura central. L'étang du Lautrey (France), C. R. Acad. Sci. Paris, Ser. IIa 325 (1997) 43–48.

[5] J.F. Buoncristiani, M. Campy, Expansion and retreat of the Jura ice sheet (France) during the Last Glacial Maximum: Sediment, Geol. 165 (2004) 253–264.

[6] D. Calmels, Altération chimique des carbonates : influence des sources d'acidité sur les bilans globaux, Ph.D. thesis, Université Paris Diderot, 2007, 228 p.

[7] C. Cupillard, M. Magny, H. Richard, P. Ruffaldi, S. Marguier, Mésolithisation et néolithisation d'une zone de moyenne montagne: évolution du peuplement et du paysage de la haute vallée du Doubs, C.R. de fin de projet, Laboratoire de Chrono-écologie, Besançon, 1994, 120 p.

[8] J.-L. de Beaulieu, V. Andrieu-Ponel, R. Cheddadi, F. Guiter, C. Ravazzi, M. Reille, S. Rossi, Apport des longues séquences lacustres à la connaissance des variations des climats et des paysages pléistocènes, C. R. Palevol 5 (2006) 65–72.

[9] I. Hajdas, S.D. Ivy-Ochs, G. Bonani, A.F. Lotter, B. Zolitschka, C. Schluchter, Radiocarbon age of the Laacher See Tephra: 11 230 ± 40 BP, Radiocarbon 37 (1995) 149–154.

[10] H. Holzhauser, M. Magny, H.J. Zumbühl, Glacier and lake-level variations in West-Central Europe over the last 3500 years, Holocene 15 (2005) 789–801.

[11] E. Juvigné, S. Kozarski, B. Nowaczyk, The occurrence of Laacher See Tephra in Pomerania, NW Poland, Boreas 24 (1995) 225–231.

[12] C.H. Langmuir, R.D. Vocke Jr., G.N. Hanson, S.R. Hart, A general mixing equation with applications to Icelandic basalts: Earth Planet, Sci. Lett. 37 (1978) 380–392.

[13] M. Magny, Palaeohydrological changes as reflected by lake-level fluctuations in the Swiss Plateau, the Jura Mountains and the northern French Pre-Alps during the Last Glacial-Holocene transition: a regional synthesis, Glob. Planet. Change 30 (2001) 85–101.

[14] M. Magny, G. Aalbersberg, C. Begeot, P. Benoit-Ruffaldi, G. Bossuet, J.-R. Disnar, O. Heiri, F. Laggoun-Defarge, F. Mazier, L. Millet, O. Peyron, B. Vanniere, A.-V. Walter-Simonnet, Environmental and climatic changes in the Jura Mountains (eastern France) during the Lateglacial-Holocene transition: a multi-proxy record from Lake Lautrey, Quat. Sci. Rev. 25 (2006) 414–445.

[15] H.W. Nesbitt, G.M. Young, Prediction of some weathering trends of plutonic and volcanic rocks based on thermodynamic and kinetic considerations, Geochim. Cosmochim. Acta 48 (1984) 1523–1534.

[16] W. Pennington, R.S. Cambray, J.D. Eakins, D.D. Harkness, Radionuclide dating of the recent sediment using fallout ^{137}Cs as a tracer, Nature 242 (1976) 324–326.

[17] O. Peyron, C. Begeot, S. Brewer, O. Heiri, M. Magny, L. Millet, P. Ruffaldi, E. Van Campo, G. Yu, Late-Glacial climatic changes in eastern France (Lake Lautrey) from pollen, lake-levels, and chironomids, Quat. Res. 64 (2005) 197–211.

[18] M. Pochon, Origine et évolution des sols du Haut Jura suisse, Mémoires de la Société helvétique des Sciences Naturelles 110, 1978, 190 p.

[19] P.J. Reimer, K.A. Hughen, T.P. Guilderson, G. McCormac, M.G.L. Baillie, E. Bard, P. Barratt, J.W. Beck, C.E. Buck, P.E. Damon, M. Friedrich, B. Kromer, C.B. Ramsey, R.W. Reimer, S. Remmele, J.R. Southon, M. Stuiver, J. Van der Plicht, Preliminary report of the first workshop of the intcal04 radiocarbon calibration/comparison working group, Radiocarbon 44 (2002) 653–661.

[20] A. Schwalb, P. Hadorn, N. Thew, F. Straub, Evidence for Late Glacial and Holocene environmental changes from subfossil assemblages in sediments of Lake Neuchatel, Switzerland, Palaeogeogr, Palaeoclimatol. Palaeoecol. 140 (1998) 307–323.

[21] F.B. Smith, M.J. Clark, Radionuclide deposition from the Chernobyl cloud, Nature 322 (1986) 690–691.

[22] S.J. Ursic, F.D. Dendy, Sediment yields from small watersheds under various land uses and forest covers, in: U.S. Dep. of Agric. (Ed), Federal Inter-Agency Sedimentation Conference 970 (1965) 7–52.

[23] P.P. Van Der Bogaard, Laacher See tephra: a widespread isochronous Late Quaternary tephra layer in central and northern Europe: Geol, Soc. Am. Bull. 96 (1985) 1554–1571.

[24] A.-V. Walter-Simonnet, G. Bossuet, A.-L. Develle, C. Bégeot, P. Benoît-Ruffaldi, M. Magny, T. Adatte, J.-P. Simonnet, M. Rossy, B. Vannière, M. Thivet, L. Millet, B. Régent, C. Wackenheim, Chronologie et spatialisation de retombées de cendres volcaniques Tardiglaciaires dans les massifs des Vosges et du Jura, et le plateau suisse, Quaternaire 19 (2008) 117–132.

[25] M. Wessels, Natural environmental changes indicated by Late Glacial and Holocene sediments from Lake Constance, Germany, Palaeogeogr. Palaeoclimatol. Palaeoecol. 140 (1998) 421–432.